Engineering Structures 48 (2013) 281–291

Contents lists available at SciVerse ScienceDirect

Engineering Structures

journal homepage: www.elsevier.com/locate/engstruct

Effect of local damage on the behavior of a laboratory-scale steel truss bridge

Garrett Brunell [a], Yail J. Kim [b,*]

[a] Ulteig, Minneapolis, MN 55421, USA
[b] Department of Civil Engineering, University of Colorado Denver, Denver, CO 80217, USA

ARTICLE INFO

Article history:
Received 13 August 2012
Revised 13 September 2012
Accepted 14 September 2012
Available online 24 November 2012

Keywords:
Damage
Truss
Redundancy
Safety index

ABSTRACT

This paper presents an investigation into the performance of a steel truss bridge subjected to local damage. An experimental program with 16 damage scenarios is conducted to study the behavior of damaged truss systems. A three-dimensional numerical model is developed to predict the test results. Static and dynamic responses of the damaged trusses are compared with those of the control. Various technical aspects are studied, including damage quantification using a damage index, load rating, variation of strain energy, modal analysis, and structural safety based on simple reliability theory. Service performance of the truss bridge is significantly influenced by local damage (i.e., damage index >0.5) and the load-carrying capacity is exponentially reduced with the increased damage index. A high mode shape such as the 4th mode is of use to diagnose local damage in the truss system. The global safety index derived using deflection characteristics is an indicator to indirectly detect the presence of local damage in the system. Stress redistribution among the constituent truss members is found to be insignificant, except for those adjacent to the damage. The global safety index of the system based on deflection characteristics is an indicator to diagnose the presence of local damage. The need for developing a repair method that can address the global redundancy of a damaged truss bridge is highlighted.

1. Introduction

Deterioration of bridge infrastructure is a critical concern over the world. According to the American Society of Civil Engineers [1], the average age of bridges in the US is 43 years old as of 2010 and an overall grade of C was given to these bridges. Correspondingly, over 25% of bridges in the nation are classified as structurally deficient or functionally obsolete. Bridges classified by one of these two categories do not operate at their required capacity and require restrictions which impede the public's use of the bridge. Government agencies spend significant expenditures for timely maintenance and rehabilitation to address these issues. In many cases, bridge insufficiencies can be attributed to aging, environmental damage, higher levels of demand and load being realized by bridges than what they were initially designed for, greater amounts of deicing agents in use, and shortfalls in the initial design. In addition to numerous bridges not meeting current standards, catastrophic bridge failure events such as the I-35 collapse in Minneapolis, MN, have generated an increased level of attention towards the issues associated with existing bridges. Hao [2] reported that the I-35W bridge had collapsed because of excessive stresses accumulated in local members: inadequate gusset plate design thickness and member side wall thickness which were insufficient to support service load.

Effort has been made on studying the behavior of constructed truss bridges. Lenett et al. [3] conducted an inspection project on a three-span truss bridge between Ironton, Ohio and Russell, Kentucky. The states of existing and repaired truss members were visually examined. Strain responses of selected members were monitored when subjected to known truck loads. Inspection data provided crucial information to the rating and posting of the bridge. Azizinamini [4] performed a full-scale load test using a decommissioned truss bridge. Load-carrying capacity of the bridge was experimentally determined and the mode of failure was observed. Local failure of a diagonal tension member initiated abrupt failure of the truss system, highlighting that attention should be paid to the local behavior of tension members in aged truss bridges. Alampalli and Kunin [5] examined the interaction between the deck and truss system of a rehabilitated 50-year old bridge. Several load combinations with heavy trucks were used to measure the response of the bridge. Test results indicated that the response of the bridge deck was affected by the local behavior of truss members. Hickey et al. [6] tested a 260 m truss bridge situated between Pulaski and Hillsville, Virginia using two 25 ton trucks. Deflections and strains were measured and a numerical model was developed to predict the test data. Findings included that the bridge's response was characterized by floor beams and

* Corresponding author.
E-mail address: jimmy.kim@ucdenver.edu (Y.J. Kim).

0141-0296/$ - see front matter © 2012 Elsevier Ltd. All rights reserved.
http://dx.doi.org/10.1016/j.engstruct.2012.09.017

stringers, and that local failure of truss members was a critical consideration.

More specific to truss bridges from a structural redundancy perspective, Frangopol and Curley [7] identified that truss bridges were often classified as either multiple load path (*fail-safe* structures) or single load path (*weakest-link* structures). The type of classification depends on the structure's ability to find suitable alternative load paths when damage is present. Structures that are classified as *weakest-link* lack system redundancy and therefore when subject to damage become increasingly more susceptible to failure. Ghosn and Moses [8] proposed methodologies to examine the level of redundancy in existing truss bridges. Several limit states were defined based on ultimate, service, and damage configurations. System factors were suggested to evaluate structural redundancy and preliminary design provisions were discussed. Nagavi and Aktan [9] categorized trusses as either a *light* or *heavy* classification. A truss system categorized into the *light* class was composed of pin-ended, solid bar, tension members, and small rolled shapes for compression members, while a system classified as the *heavy* class was assembled from members of only hot rolled shapes and connected by riveted gusset plates. Differences in performance between these two classes were predominantly due to the pin-ended connection in the *light* class truss where a lack of redundancy created a greater failure potential. Kim and Yoon [10] stated that a lack of redundancy in steel truss bridges could cause susceptibility to premature failure. This is because truss bridges are generally considered to be a non-redundant system as the failure of a single component often leads to the successive failure of multiple components and ultimately the failure of the entire system.

As discussed above, the global response of a truss bridge is significantly influenced by the local behavior of constituent members. Most research is concerned with non-destructive load tests on truss bridges and corresponding responses. Limited information is available regarding the effect of local damage on the behavior of a truss system and experimental investigations are particularly rare. This paper presents an experimental study to examine the response of a scaled truss bridge having various damage scenarios. A three-dimensional numerical model was developed and validated with test data. The model was further used to expand laboratory findings. A simple reliability analysis was carried out to evaluate the performance of damaged truss bridges.

2. Research significance

Truss bridges intrinsically lack structural redundancy when compared to slab-on-girder bridges. Reliability of such a system is significantly influenced by local damage due to the alteration of load path. A catastrophic event may take place if increased distress exceeds the capacity of a damaged system. The effect of local damage on the behavior of a truss bridge needs further research. Current practice and design standards for truss bridges do not explicitly take into consideration the interaction between constitutive members and global response. These facts create the need to study the effects that damage has on steel truss bridges. Although a few numerical investigations have been conducted to examine the behavior of damaged truss bridges [2,8], experimental effort has been limitedly reported. Of primary concern of this laboratory investigation combined with a modeling approach is the change in response of steel truss bridges from intact to damaged conditions, including static and dynamic behavior.

3. Experimental program

3.1. Material and truss system

A deck-truss bridge scaled to 1:20 (L = 6.2 m) was designed using different sizes of steel tubes (Grade A36), as shown in Fig. 1. Similar scale laboratory bridges were tested previously [11–13]. Given highway bridges show elastic behavior in service load, the scaled bridge having adjustable web members was able to simulate various types of damage within an elastic load range (to be discussed). The material and bridge dimensions are displayed in Fig. 1a. The truss system consisted of two main trusses (Trusses 1 and 2), lateral stiffening frames (secondary truss elements) welded along the top chord of each truss to provide a stable test environment, cross braces, and leg members. Several pieces of truss parts comprising these elements were fabricated to form a complete set of the designed truss bridge (Fig. 1b). The number of cross braces was minimized during design by addition of the lateral frame that would prevent buckling of the top chord on each truss. The primary role of the brace members was to maintain stability of the system when loaded. Steel components included the following nominal properties: yield stress (σ_y) = 290 MPa, elastic modulus (E) = 200 GPa, and Poissons ratio (υ) = 0.3.

3.2. Damage simulation

Damage simulations were generated by removing web elements from the truss. As mentioned in Section 1, local damage in diagonal members is an important consideration. Fig. 2a provides a schematic view of damage configurations. To represent significant damage in constructed truss bridges, a set of four adjacent elements was removed per damage scenario, as typically shown in Fig. 2b. It is worthwhile to note that laboratory research frequently assumes more severe damage than that could happen on site [14–16]. A total of 16 damage combinations were designed, depending upon the location of damaged elements (Table 1). An identification code for each damage scenario indicated the location of damage in either Truss 1 or 2, and the position of the damage within the truss (positions 1, 2, 3, and 4, as shown in Fig. 2a). For example, Specimen 1_1 denotes that the location of damage was in Truss 1 with position 1, while Specimens 1_2 and 2_3 calls out Truss 1 with damage position 2 and Truss 2 with damage position 3.

3.3. Loading and instrumentation

The truss system was monotonically loaded at a typical service load of 4.5 kN (i.e., 25% of the predicted capacity of the control truss). Each test category was loaded five times to ensure the reproducibility of experimental results. A 25 mm thick steel grate (915 mm × 1015 mm) was used near midspan of the truss, as shown in Fig. 1c. To achieve a uniform distribution of load from the hydraulic actuator along the length of the grate, a steel channel was centered at the middle of the grate and spanned the length of the grate. Deflection of the test truss was recorded by linear potentiometers located at midspan of the truss. Strain gages were bonded to selected members in order to measure axial behavior (Fig. 1a). Structural responses of the control truss and each damage scenario were recorded using the Dataq data acquisition system.

4. Numerical modeling

Modeling the truss bridge was performed using RISA 3-D structural analysis software. A complete three-dimensional model of the bridge was used for analysis, including two single span trusses, three cross braces, and four piers, as shown in Fig. 3. The respective element cross section geometries were input into the software's material database where the cross sectional properties were calculated. Boundary conditions were established at the base of each pier. The degrees of freedom that were restrained at each pier included translation in the longitudinal, lateral, and vertical directions. It should be noted that the pier element was rigidly

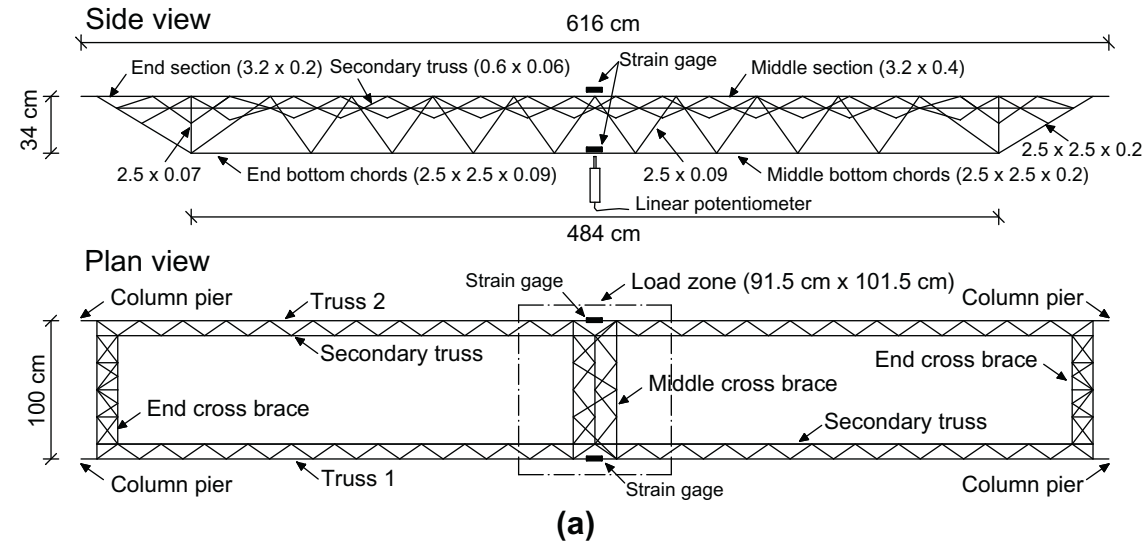

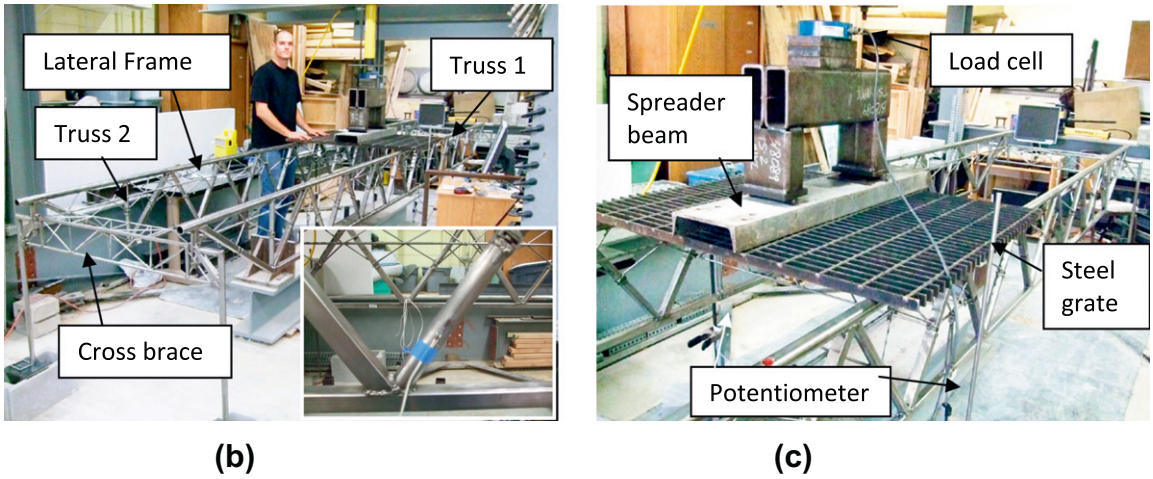

Fig. 1. Truss details: (a) truss members; (b) fabricated truss system and connection; (c) loading and instrumentation.

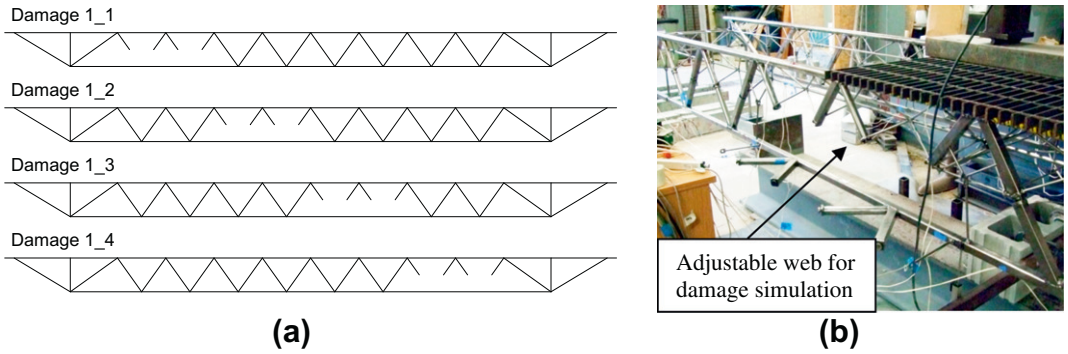

Fig. 2. Damage scenario: (a) identification of damage position; (b) simulated damage (Specimen 2 with damage position 1_2).

connected to the truss members so that the system became statically stable as in the case of the experimental specimen. Upon generation of members in RISA, finite elements were automatically sub-meshed. In total, 404 line elements and 250 nodes were used to generate the control truss. Fixed connectivity was used at all element connections in the truss model, as in the experimental truss (Fig. 1b). Material properties were input based on the values mentioned in Section 3. The load used in the test program (4.5 kN) was spread along the top truss chord where the steel grate was positioned (Fig. 1c), as a distributive line load.

Table 1
Specimen details and damage index.

Specimen ID	Damage scenario	Damage index					
		Truss 1			Truss 2		
		Exp[a] (a)	Model (b)	Margin[b] (%)	Exp[a] (a)	Model (b)	Margin[b] (%)
Control	None	N/A	N/A	N/A	N/A	N/A	N/A
1	1_1	0.52	0.62	19.2	0.09	0.01	88.9
2	1_2	0.39	0.49	25.6	0.12	0.01	91.7
3	1_3	0.41	0.49	19.5	0.04	0.01	75.0
4	1_1 and 1_3	0.60	0.72	20.0	0.01	0.02	100.0
5	1_1 and 1_4	0.65	0.76	16.9	0.05	0.03	40.0
6	1_1 and 2_1	0.58	0.63	8.6	0.60	0.63	5.0
7	1_1 and 2_2	0.51	0.63	23.5	0.50	0.49	2.0
8	1_1 and 2_3	0.52	0.62	19.2	0.53	0.49	7.5
9	1_1 and 2_4	0.56	0.63	12.5	0.65	0.63	3.1
10	1_2 and 2_2	0.38	0.49	28.9	0.41	0.49	19.5
11	1_2 and 2_3	0.37	0.49	32.4	0.45	0.49	8.9
12	1_1, 2_1 and 2_3	0.59	0.63	6.8	0.73	0.72	1.4
13	1_1, 2_1 and 2_4	0.62	0.63	1.6	0.76	0.77	1.3
14	1_2, 2_1 and 2_3	0.45	0.49	8.9	0.69	0.72	4.3
15	1_2, 2_1 and 2_4	0.57	0.49	14.0	0.77	0.77	0.0
16	1_3, 2_1 and 2_3	0.49	0.49	0.0	0.71	0.72	1.4

[a] Average value of measured test data.
[b] Margin (%) = absolute value of $(a - b)/a \times 100$.

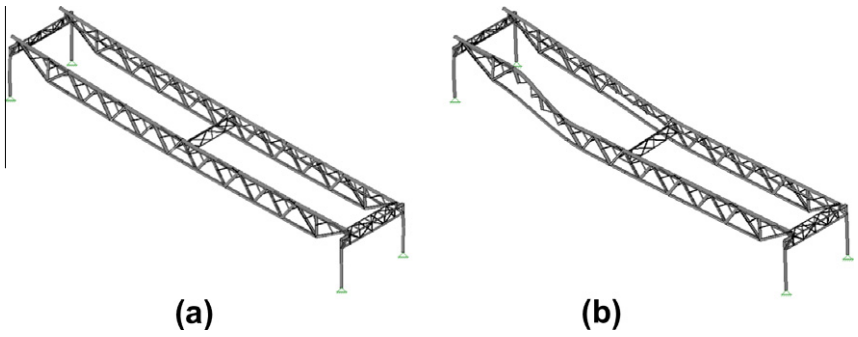

Fig. 3. Numerical model showing deflection at 20 times magnification for the service load of 4.5 kN: (a) control truss; (b) damaged truss (Specimen 7).

5. Test results and model prediction

5.1. Static behavior

5.1.1. Damage index

To quantify the behavior of the damaged truss systems, a damage index (DI) was used:

$$DI = 1 - \frac{k'}{k} \tag{1}$$

where k and k' are the stiffness of the control and damaged trusses, respectively. The stiffness of each truss was obtained from the ratio of applied load to corresponding deflection at midspan. It should be noted that use of a damage index is more relevant than a comparison employing a load versus deflection response because the applied load to the truss specimens was in an elastic range. Table 1 presents the measured and predicted damage indices, including average margins of 16.1% and 28.1% for Trusses 1 and 2, respectively. Substantially high margins were noticed for Truss 2 when the primary damage was present in Truss 1 (Specimens 1–5 as shown in Table 1). Such an observation illustrates that the load distribution between experimental Trusses 1 and 2 was not even when one of these trusses was damaged (i.e., the loading elements and trusses were not physically connected in the test), which was different from the ideal load distribution in numerical counterparts. This is confirmed by the reduced margins of Specimens 12–16 (3.9% on average) where damage occurred in both trusses. Individual stiffness responses of the predictive models were consistently greater than those measured (i.e., rigid shift). The reason is attributed to the fact that the test truss system was the assembly of several truss segments (further discussions are available later).

Fig. 4a shows the relationship between the damage index and the normalized deflection at midspan (i.e., deflection of a damaged truss divided by that of the control at a load of 25% of the control capacity). A gradual increase in the normalized deflection was observed when the damage index increased. Note that all experimental trusses were modeled and corresponding predictions were connected without markers in Fig. 4a to avoid confusion with the test data. Predicted results exhibited good agreement with the test data, including an average error of 12%. These results indicate that local damage in a truss system considerably influenced the serviceability of the system, particularly critical when a damage index was greater than 0.5. Similarly, a relationship between the damage index and predicted failure load was developed in Fig. 4b. The load at failure was defined by the load when the most stressed truss member reached its yield capacity [6]. Fig. 4b shows that the predicted ultimate load exponentially decreased with an increased damage index. For example, the control truss experienced a failure load of 18.7 kN, while at a damage index of 0.76 a failure load of 6.3 kN (i.e., 33.7% of the control capacity) was observed. These results imply that the degree of damage severity abruptly influences

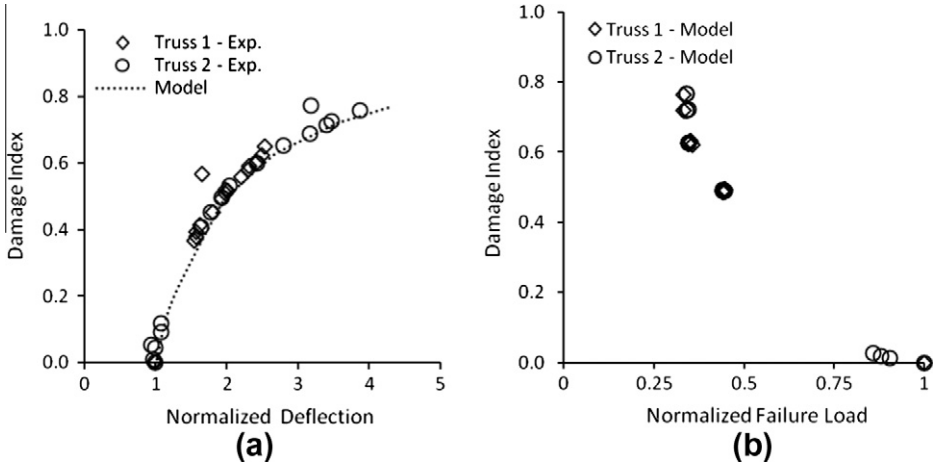

Fig. 4. Effect of damage level on performance of truss: (a) normalized deflection; (b) normalized failure load.

the response of a truss system. Such a trend explains why truss systems collapse in a sudden manner without a warning of impending failure.

5.1.2. Strain response

Fig. 5 compares the measured and predicted member strains at midspan (presented here for brevity are the top and bottom chords for the control and damaged trusses 1 and 7). Strain response of all experimental specimens was basically linear and the recorded strain values were considerably lower than the yield strain of A36 steel ($\varepsilon_y = 0.0015$). These observations ensured that multiple damage scenarios using a single truss system (Table 1) were adequately conducted without the presence of plastic damage in the system. The experimental load–strain responses tended to be stiffer than those predicted. This can be explained by the initial incomplete engagement of all connections: the truss system was assembled with several truss segments and the system required slight adjustment in each connection when loaded, which influenced the response (i.e., strain readings) of the experimental truss.

5.1.3. Rating of damaged truss system

Load rating of the damaged truss systems was conducted using the method shown in the *Manual for Condition Evaluation of Bridges* [17]:

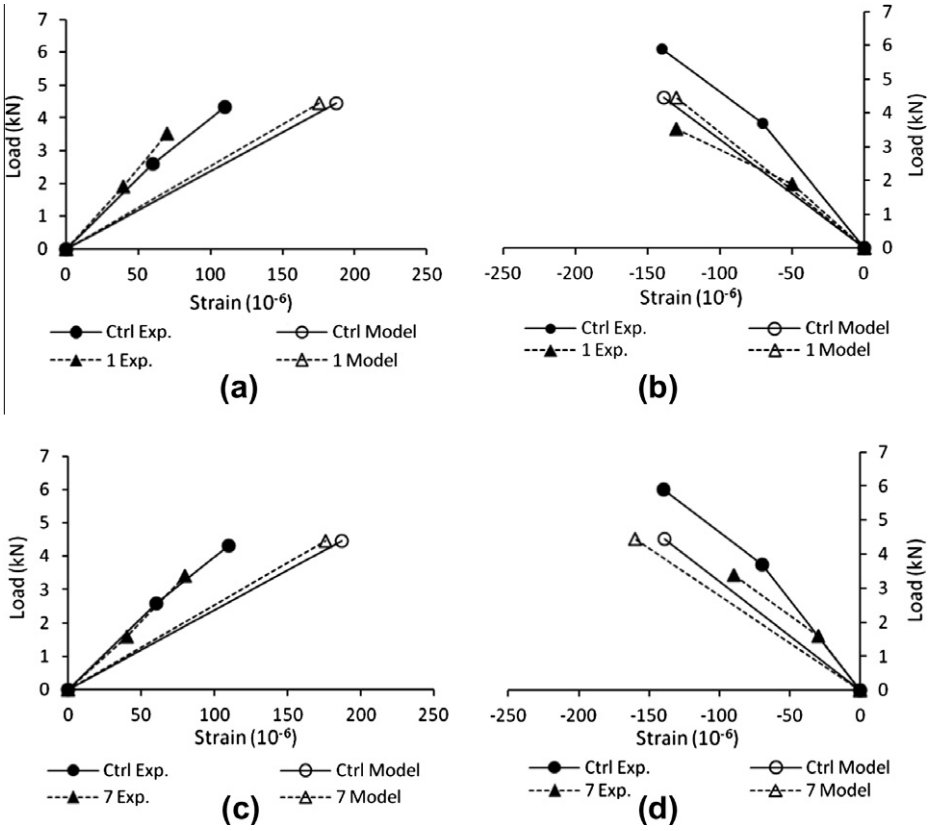

Fig. 5. Strain response: (a) Specimen 1 – Truss 1 bottom chord; (b) Specimen 1 – Truss 1 top chord; (c) Specimen 7 – Truss 1 bottom chord; (d) Specimen 7 – Truss 1 top chord.

$$RF = \frac{C - A_1 D}{A_2 L(1 + I)} \tag{2}$$

where RF is the rating factor consisting of *Operating* and *Inventory* ratings; C is the predicted capacity of the truss system; D and L are the dead and live load effects, respectively; A_1 and A_2 are the factors for the dead and live loads, respectively; and I is the impact factor. For Operating rating, A_1 and A_2 are 1.3 and 1.3, respectively, while for Inventory rating these are 1.3 and 2.17, respectively. The impact factor for the present truss systems was set to 0.1 by assuming smooth approach and deck conditions [18]. It should be noted that use of the impact factor can generate a more realistic rating for constructed truss bridges even though such an impact factor has not been presented in the test trusses. The truss capacity for each scenario was taken as the load that initiated first yielding of a member; the dead load was taken as the self weight of the bridge, 0.77 kN; and the live load was the service load of 4.5 kN. Fig. 6 compares the rating factors of each damaged truss using the Operating and Inventory ratings (Fig. 6a and b, respectively). Relatively constant rating factors were observed for Truss 1 because it was primarily damaged in all damage scenarios, as shown in Table 1 and Fig. 2a. The rating of Truss 2 was, however, fluctuating due to their inconsistent damage location. The rating factors of Truss 2 in Specimens 1–5 were 63% higher than those of Truss 1, on average, for the Operating and Inventory. These results illustrate that load transfer between these two trusses was not significant when only one truss was damaged because a concrete deck slab connecting these two members was not included in this study. Fig. 7a shows the relationship between the rating factors and the ratio of service deflection to ultimate (failure) deflection. The relationship exhibits that as the predicted rating factor decreases the service deflection approaches the failure deflection at an increasing rate. The rate of change in the normalized deflection for Operating and Inventory was similar to each other. For instance, the changes in the Operating and Inventory ratings for Truss 1 were 57.1% and 58.8%, respectively, when the normalized deflection increased from 0.26 to 0.55, as shown in Fig. 7a. Fig. 7b compares the damage index with the failure load of the damaged trusses when normalized to the failure load of the control truss. The damage index of the truss systems was found to be less than 0.4 to maintain an Inventory rating factor (representing vehicle loads being safely operated for an indefinite period of time) equal to or greater than 1.5 that were associated with a normalized failure load of 0.9. Given the purpose of the current rating analysis was to demonstrate the effect of local damage on the response of damaged truss bridges, the specific values presented above may not be directly used in practice.

5.1.4. Strain energy

To analyze force redistribution resulting from local truss damage, the element strain energy of a damaged truss was normalized against the strain energy of the control by the following:

$$U_n = \frac{U_{i-damaged}}{U_{i-control}} \quad \text{in which} \quad U_i = \frac{P^2 L}{2AE} \tag{3}$$

where U_n is the normalized element strain energy; U_i is the strain energy of the truss; A and L are the cross-sectional area and length of the members, respectively; P is the member force; and E is the elastic modulus of the member. Fig. 8 depicts that member proximity to damage is a key factor on the performance of truss components. For example, the strain energy of Member M1_6 increased roughly 3.5 times more than that of other members (i.e., M1BCA_1 and M1_17) because M1_6 was directly adjacent to damage for the majority of the damage scenarios (except when M1_6 was removed or when scenario 1_3 or 1_4 was tested). Such an observation indicates that the stress of a damaged truss member may not be effectively redistributed to other members except for those located near the damage. A catastrophic failure event of a truss system can thus initiate at the critical region. This conclusion highlights the need for improving the redundancy of a damaged truss system, rather than localized element-level repair, so that the overall performance of the truss can be enhanced.

5.2. Dynamic behavior

Dynamic analysis of a predictive model may be reasonably performed once the model has been validated with static conditions [19]. The following discusses the predicted dynamic behavior of the truss systems subjected to the same live load criteria used for the static investigations. It should be noted that the purpose of this dynamic analysis was to examine the natural frequencies and corresponding modes of the truss bridges, rather than to study the behavior subject to dynamic load.

5.2.1. Mode shape

Mode shapes of the control and damaged trusses were generated and the equivalent mode shapes were compared to one another. Figs. 9 and 10 show the first four modes for the control truss and Specimen 9 that represents a typical damaged truss system studied here. The shape of modes 1 and 2 was observed to be independent of the level of damage; however, variance between the control and damaged trusses was present at higher modes. For the control truss, modes 1 and 2 displayed lateral sway (Fig. 9a) and longitudinal shift (Fig. 9b), respectively, while modes

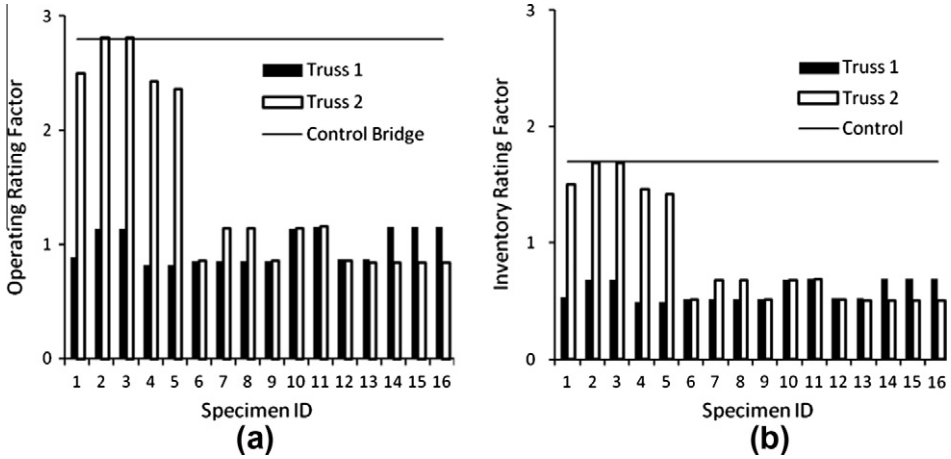

Fig. 6. Load rating of predicted truss systems for Trusses 1 and 2: (a) Operating rating; (b) Inventory rating.

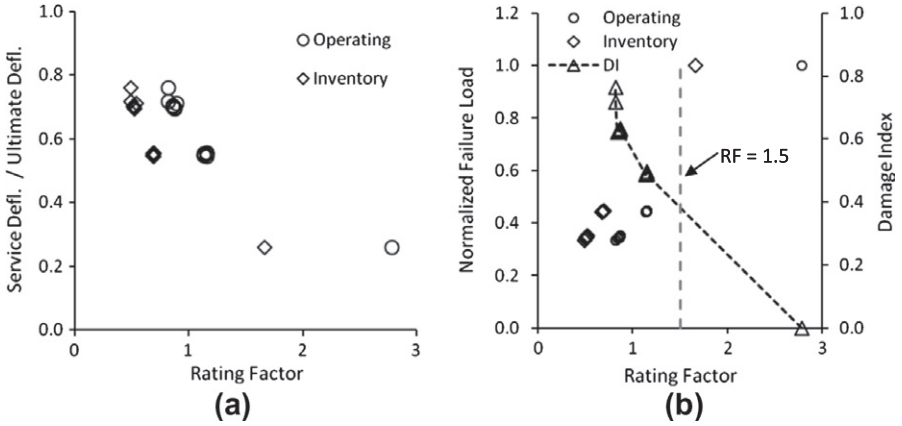

Fig. 7. Load rating versus predicted performance of damaged truss systems (Truss 1): (a) deflection; (b) failure load.

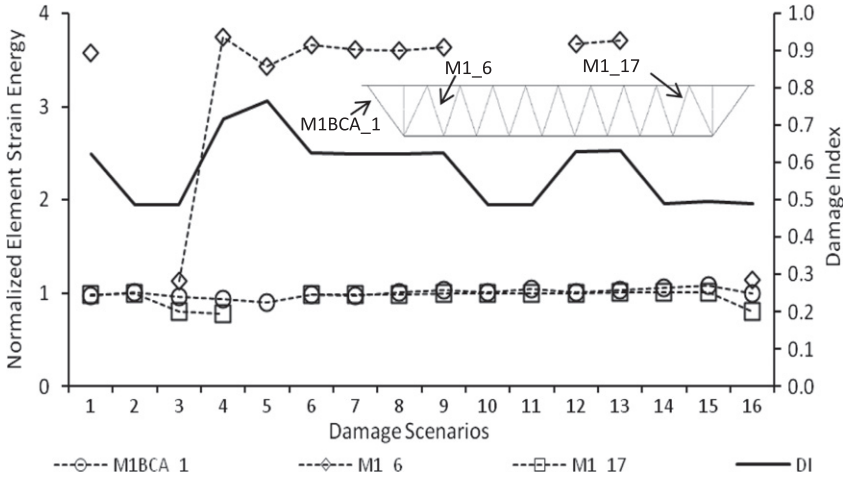

Fig. 8. Comparison of the normalized strain energy for three tension members.

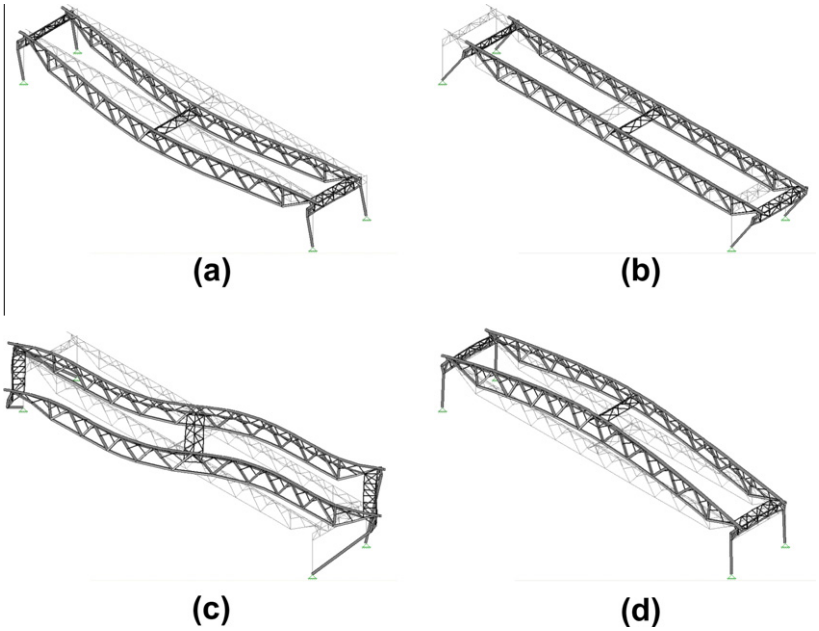

Fig. 9. Mode shape of control truss during service load level of 4.5 kN: (a) mode 1, (b) mode 2, (c) mode 3, and (d) mode 4.

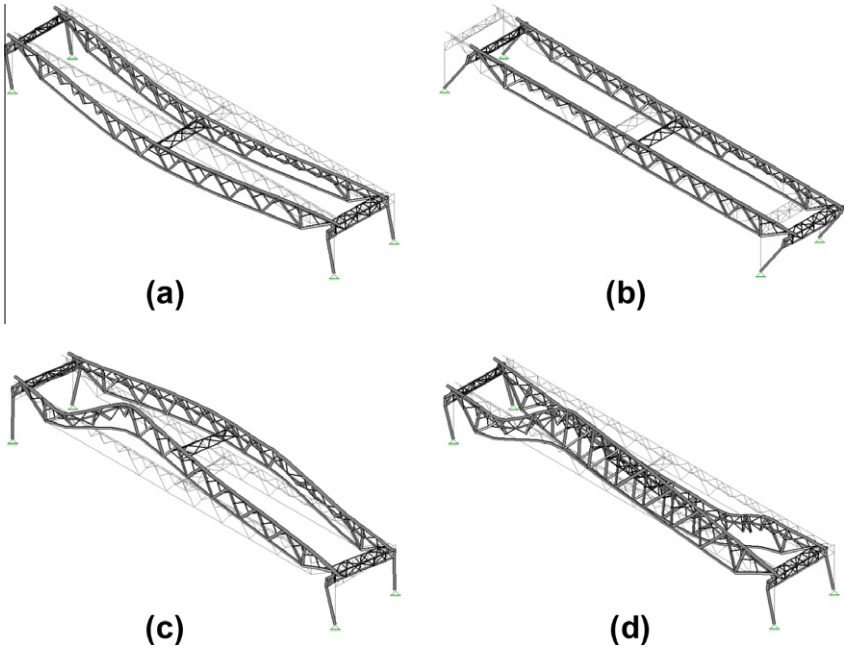

Fig. 10. Mode shapes of Specimen 9 during service load level of 4.5 kN: (a) mode 1, (b) mode 2, (c) mode 3, (d) mode 4.

3 and 4 demonstrated twist about the center of the truss (Fig. 9c) and camber (Fig. 9d), respectively. Mode shapes 1 and 2 of the damaged truss (Specimen 9) were the same as those of the control (Fig. 10a and b), whereas modes 3 and 4 lacked the symmetry and direction of deformation that the control mode shape exhibited, as respectively shown in Fig. 10c and d. Such distinct changes in mode shapes of the damaged truss are attributed to the reduced stiffness in the direction of displacement. The sensitivity of higher modes was confirmed by the changes in frequency discussed in the following section.

5.2.2. Frequency

Damage detection by changes to resonant frequencies may be useful because they are reliable and quickly obtainable. This method of damage detection is based on the principle that structural frequency (f) is directly related to the equivalent stiffness of the structural system (k_e) and inversely related to the mass (m):

$$f = \frac{1}{2\pi}\sqrt{\frac{k_e}{m}} \tag{4}$$

A decrease in resonant frequency signifies a loss of stiffness and therefore damage to the system. However, changes in frequency greater than 5% are the only way to be sure that damage is present as long as these measurements are not subject to changes in ambient conditions [20]. Table 2 summarizes the frequencies of the damage scenario modes corresponding to the first four modes of the control bridge. It is important to note that mode shapes which demonstrate similar deformation should be compared so that an accurate measure for the change in modal frequency is achieved. From a comparison of the control truss to the damaged counterparts, modes 1, 2, and 3 showed negligible change in frequency (less than 3.0%) with changes to the degree of damage present. Mode 4, on the other hand, demonstrated much greater changes to frequency from the control to damaged cases. Mode 4 readily detected changes in frequency from 28.9% (Specimens 2 and 3) to 50.4% (Specimens 13 and 15), indicating that this is a recommended mode to diagnose the presence of damage in the truss systems studied here. Fig. 11 shows the change in natural frequency of the system for modes 1–4 with respect to the worst-case damage index of Trusses 1 and 2. As discussed above, modes 1–3 had little to no effect on the natural frequency; however, the frequency of mode 4 remarkably decreased with an increased damage index. This implies that the use of natural frequency associated with a higher order mode shape (i.e., 4th mode in this study) is a quantifiable indicator of damage, thereby a meaningful tool for damage inspection of constructed truss bridges.

Table 2
Modal frequencies of truss specimens.

Specimen ID	Mode and frequency							
	1		2		3		4	
	Hz	Δ^a (%)	Hz	Δ^a (%)	Hz	Δ^a (%)	Hz	Δ^a (%)
Control	0.94	–	1.41	–	5.28	–	8.17	–
1	0.94	0.4	1.41	0.1	5.29	−0.1	5.09	37.7
2	0.94	0.4	1.41	0.1	5.21	1.3	5.81	28.9
3	0.94	0.4	1.41	0.1	5.21	1.3	5.81	28.9
4[b]	0.94	0.7	1.41	0.1	5.22	1.2	4.38	46.4
5[b]	0.94	0.7	1.41	0.1	5.29	−0.1	4.06	50.3
6[b]	0.94	0.7	1.41	0.1	5.18	2.0	4.99	38.9
7[b]	0.94	0.7	1.41	0.1	5.22	1.2	5.08	37.8
8[b]	0.94	0.7	1.41	0.1	5.22	1.1	5.07	37.9
9[b]	0.94	0.7	1.41	0.1	5.29	−0.2	4.99	38.9
10	0.94	0.7	1.41	0.1	5.13	3.0	5.74	29.7
11	0.94	0.7	1.41	0.1	5.13	2.9	5.72	30.0
12[c]	0.93	1.1	1.41	0.1	5.23	0.9	4.36	46.6
13[c]	0.93	1.1	1.41	0.1	5.29	−0.2	4.05	50.4
14[b]	0.93	1.1	1.41	0.1	5.13	2.9	4.37	46.5
15[b]	0.93	1.1	1.41	0.1	5.22	1.2	4.05	50.4
16[b]	0.93	1.1	1.41	0.1	5.13	2.8	4.37	46.5

Note: frequencies shown in table for damage scenarios are frequencies of modes corresponding to the first four modes of the control bridge. The changes in mode are noted by; b or c.

[a] Difference between control and damaged truss.
[b] Mode 3 switches with mode 4.
[c] Mode 3 is mode 4 and mode 5 is mode 3.

6. Reliability analysis

6.1. Safety index

A deflection-based safety index was used to quantify the performance of the damaged truss systems:

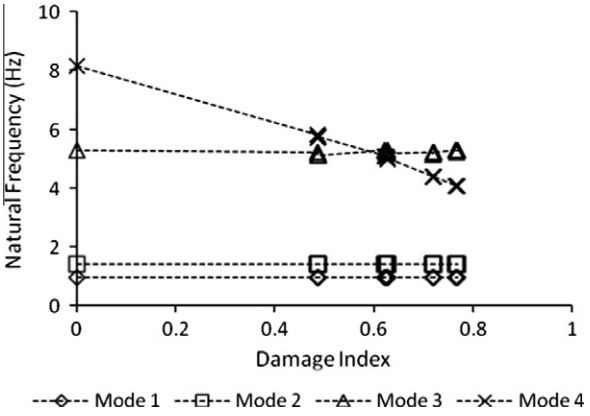

Fig. 11. Natural frequency response with the worst case damage index.

$$Z = \frac{\delta_{ult} - \delta_{serv}}{\sqrt{[\sigma(\delta_{ult})]^2 + [\sigma(\delta_{serv})]^2}} \tag{5}$$

where Z is the global safety index; and δ_{ult} and δ_{serv} are the ultimate and service deflections, respectively; and $\sigma(\delta_{ult})$ and $\sigma(\delta_{serv})$ are their standard deviations. As discussed previously, the ultimate and service deflections were respectively obtained when the first truss member of the model reached its yield capacity and when a service load of 4.5 kN was applied (25% of the control bridge's ultimate capacity). The proposed safety index is fundamentally aligned with the classical concept of a strength-based reliability index using the ultimate and service loads [7]. Such a deflection-based limit state has been used in NCHRP 406 [8] and accounts for the chance of approaching the ultimate deflection when service deflections increase. The coefficient of variation was taken from previous research [21,22]: 0.12 and 0.18 for the ultimate state that is related to strength and the service state that is associated with a live load effect, respectively. It should be noted that the measured coefficients of variation in the laboratory were much less than those used here because the measured values were obtained in a controlled environment that might not represent in situ conditions. Relationships between the global safety index and the deflection characteristics of the damaged truss systems are shown in Fig. 12, including the normalized deflection of a damaged system to that of the control (Fig. 12a) and the service deflection normalized to the $L/800$ limit of AASHTO (Fig. 12b). The service deflection of the damaged trusses significantly increased when the safety index decreased, whereas their ultimate deflection was relatively constant, as shown in Fig. 12a. There was no difference between the service and ultimate deflections of the damaged trusses having a safety index of greater than 4 when compared to those of the control. A global safety index of 2.5 was found to be the lowest bound to satisfy the AASHTO deflection limit, as shown in Fig. 12b. It is, thus, recommended that the reliability calibration of constructed truss bridges in service be conducted with a safety index of 2.5.

Using the same approach as for the global safety index, both the average and minimum safety indices were determined based on the capacity of individual truss elements controlling the failure of the entire system. For this method, the unity capacity (UC) of the truss members was employed: the ultimate capacity of a critical member was represented by unity and thus any value less than one meant that the member had not failed yet, as shown in

$$Z_e = \frac{1 - UC}{\sqrt{[\sigma(p_{ult})]^2 + [\sigma(p_{serv})]^2}} \tag{6}$$

where Z_e is the element safety in service (i.e., 25% of the control capacity was applied here), and $\sigma(p_{ult})$ and $\sigma(p_{serv})$ are the standard deviations for the ultimate and service forces in the truss elements, respectively. Standard deviations for the member's ultimate and service capacities were evaluated using the same coefficients of variation as used for the global safety index. Fig. 13 presents the element safety index of each damage scenario. In this figure, the Control-Avg and Damage-Avg are defined as the average element safety indices for all of the truss elements in both the control and damaged trusses, while Control-Min and Damage-Min denote the minimum safety indices of the critical member of those trusses. The average change in element safety indices between the control and the damaged cases was not significant: 12.6% and 11.7% for Trusses 1 and 2, respectively, on average. The minimum indices for the damaged truss systems were, however, remarkably lower than those of the control: 64.3% and 51.0% for Trusses 1 and 2, respectively, on average. These observations confirm that damage distribution (or stress redistribution among truss members due to local damage) in a truss system was not significant and damage localization was a critical factor leading to the safety of the system. It is interesting to note that the global safety index based on the deflection of a damaged truss system (Eq. (5)) was aligned with the minimum element safety index derived from member force, as shown in Fig. 13. This correlation implies that as load is transferred to critical elements due to the presence of damage the capacity of the element with respect to safety against failure follows the

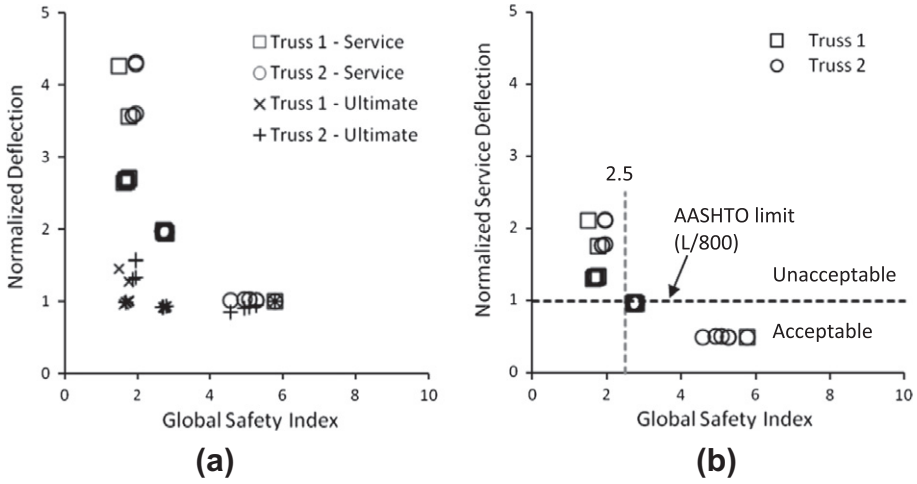

Fig. 12. Relationship between global safety index and normalized deflection: (a) to control deflection; (b) to AASHTO deflection limit.

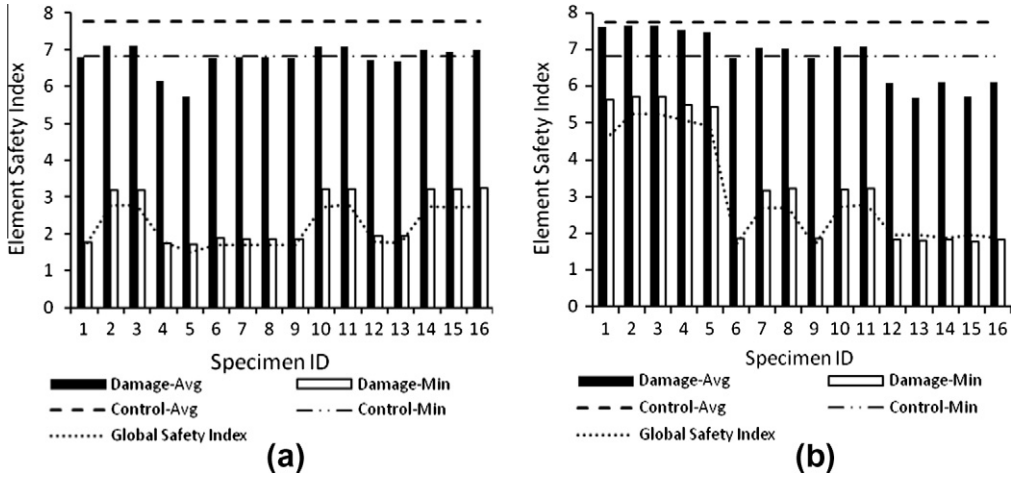

Fig. 13. Truss safety based on element safety index. (a) Truss 1; (b) Truss 2.

same trend as the deflection of the system. Regular monitoring of the deflection of an existing truss bridge is thus an important task, unless a refined health monitoring method is utilized, to indirectly estimate the progression of the minimum element safety index that represents the current state of a critical region in the bridge. This approach could be an inexpensive and practical method to determine the safety of the bridge against impending member failure.

7. Summary and conclusions

An investigation has been performed as to the effects that local damage in steel trusses has on the overall behavior of the bridge. The investigation utilized an experimental program to test a scaled model bridge, which was validated with a numerical model. The numerical modeling was then extended to investigate the relationship between damage and bridge failure. The behavior of 16 damage scenarios was compared with that of the control truss. A static analysis was carried out which utilized a damage index to quantify the level of damage present in the bridge, to examine the load transfer relationship between truss members, and to quantify the failure load for various scenarios. In addition, a dynamic analysis investigated the effect of damage on mode frequency and changes in mode shape. Given the dynamic behavior of the test specimen was not measured in the laboratory, the findings reported here could be experimentally verified in future research. A simple reliability analysis was conducted to assess the safety of the truss systems. Technical findings presented here are based on laboratory-scale research and thus a size effect might exist when implemented in practice. Another thing to note is that the technical findings reported could be conservative to a certain extent because the contribution of a reinforced concrete deck was not included. The following is concluded:

- The presence of local damage in the truss system significantly influence the serviceability of the system (i.e., deflection), particularly noticeable for those with a damage index of greater than 0.5. Load-carrying capacity of the damaged truss systems exponentially decreased with the increased damage index.
- The current AASHTO load rating method was reasonably applicable to the truss bridge system, while the rate of change in normalized deflection for the Operating and Inventory ratings was almost identical. A relationship between the damage index of the truss systems and the rating factors was established even though such a finding could not be generalized due to the limited number of model trusses.
- From a dynamic analysis perspective, a higher mode shape and corresponding frequency were useful to detect the presence of local damage in the truss systems. The natural frequency associated with the 4th mode remarkably decreased when the damage index increased, implying that the equivalent stiffness of the system was reduced in a specific direction of displacement.
- The stress of the damaged truss member was not effectively redistributed to other members, except for those adjacent to the damage. The average safety index of the constituent members was not sensitive to the local damage, whereas the safety index of the critical members was. The global safety index of the system based on deflection characteristics was a good indicator to indirectly diagnose the presence of local damage. A repair method that can improve the redundancy of a damaged truss bridge, rather than localized repair, is required to enhance the overall performance of such a bridge.

Acknowledgments

The writers gratefully acknowledge support from North Dakota State University. Special thank-you goes to the ASCE Steel Bridge Team in the Department of Civil Engineering at NDSU for their contribution to the fabrication of the experimental truss system.

References

[1] ASCE. Report card for America's infrastructure. American Society of Civil Engineers, Reston, VA; 2010.
[2] Hao S. I-35W bridge collapse. J Bridge Eng 2010;15(5):608–14.
[3] Lenett M, Hunt V, Helmicki A, Turer A. Field testing and evaluation of the Ironton–Russell truss bridge. In: Proceedings of structures congress, ASCE, Washington, DC; 2001.
[4] Azizinamini A. Full scale testing of old steel truss bridge. J Constr Steel Res 2002;58:843–58.
[5] Alampalli S, Kunin J. Load testing of an FRP bridge deck on a truss bridge. Appl Compos Mater 2003;10:85–102.
[6] Hickey L, Roberts-Wollmann C, Cousons T, Sotelino E, Easterling WS. Live load test and failure analysis for the steel deck truss bridge over the New River in Virginia. Final contract report FHWA/VTRC 09-CR8. Virginia Transportation Research Council, Charlottesville, VA; 2009.
[7] Frangopol DM, Curley JP. Effects of damage and redundancy on structural reliability. J Struct Eng 1987;113(7):1533–9.
[8] Ghosn M, Moses F. Redundancy in highway bridge superstructures (NCHRP 406). Transportation Research Board, Washington, DC; 1998.
[9] Nagavi RS, Aktan AE. Nonlinear behavior of heavy class steel truss bridges. J Struct Eng 2003;129(8):1113–21.
[10] Kim YJ, Yoon DK. Identifying critical sources of bridge deterioration in cold regions through the constructed bridges in North Dakota. J Bridge Eng 2010;15(5):542–52.

[11] Matsuda K, Cooper KR, Tanaka H, Tokushige M, Iwasaki T. An investigation of Reynolds number effects on the steady and unsteady aerodynamic forces on a 1:10 scale bridge deck section model. J Wind Eng 2001;89:619–32.
[12] Eckhoff EC, Eller VM, Watkinis SE, Hall RH. Interactive virtual laboratory for experience with a smart bridge test. In: Proceedings of the 2002 American society for engineering education annual conference and exposition, Montreal, QC, Canada; 2002.
[13] Bilello C, Bergman LA, Kuchma DK. Experimental investigation of a small-scale bridge model under a moving mass. J Struct Eng 2004;130(5):799–804.
[14] Stallings JM, Cousins TE, Stafford TE. Removal of diaphragms from three span steel girder bridge. J Bridge Eng 1999;4(1):63–70.
[15] Eamon CD, Nowak AS. Effect of secondary elements on bridge structural system reliability considering moment capacity. Struct Saf 2004;26:29–47.
[16] Shaat A, Fam A. Repair of cracked steel girders connected to concrete slabs using carbon–fiber-reinforced polymer sheets. J Compos Constr 2008;12(6):650–9.
[17] AASHTO. Manual for condition evaluation of bridges (2003 interim revisions). American Association of State Highway and Transportation Officials, Washington, DC; 2003.
[18] AASHTO. Guide specifications for strength evaluation of existing steel and concrete bridges. American Association of State Highway and Transportation Officials, Washington, DC; 1989.
[19] Zein AS, Gassman SL. Frequency spectrum analysis of impact-echo waveforms for T-beams. J Bridge Eng 2010;15(6):705–14.
[20] Salawu OS. Detection of structural damage through changes in frequency: a review. Eng Struct 1997;19(9):718–23.
[21] Nowak AS. Calibration of LRFD bridge design code. NCHRP report 12-33. Transportation Research Board, Washington, DC; 1993.
[22] Nowak AS. Calibration of LRFD bridge code. J Struct Eng 1995;121(8):1245–51.